

A Chemogenomic Screening of Sulfanilamide-Hypersensitive *Saccharomyces cerevisiae* Mutants Uncovers *ABZ2*, the Gene Encoding a Fungal Aminodeoxychorismate Lyase[∇]

Javier Botet, Laura Mateos, José L. Revuelta,* and María A. Santos

Departamento de Microbiología y Genética, Instituto de Microbiología Bioquímica, Universidad de Salamanca/CSIC, Campus Miguel de Unamuno, 37007 Salamanca, Spain

Received 25 July 2007/Accepted 5 September 2007

Large-scale phenotypic analyses have proved to be useful strategies in providing functional clues about the uncharacterized yeast genes. We used here a chemogenomic profiling of yeast deletion collections to identify the core of cellular processes challenged by treatment with the *p*-aminobenzoate/folate antimetabolite sulfanilamide. In addition to sulfanilamide-hypersensitive mutants whose deleted genes can be categorized into a number of groups, including one-carbon related metabolism, vacuole biogenesis and vesicular transport, DNA metabolic and cell cycle processes, and lipid and amino acid metabolism, two uncharacterized open reading frames (*YHI9* and *YMR289w*) were also identified. A detailed characterization of *YMR289w* revealed that this gene was required for growth in media lacking *p*-aminobenzoic or folic acid and encoded a 4-amino-4-deoxychorismate lyase, which is the last of the three enzymatic activities required for *p*-aminobenzoic acid biosynthesis. In light of these results, *YMR289w* was designated *ABZ2*, in accordance with the accepted nomenclature. *ABZ2* was able to rescue the *p*-aminobenzoate auxotrophy of an *Escherichia coli* *pabC* mutant, thus demonstrating that *ABZ2* and *pabC* are functional homologues. Phylogenetic analyses revealed that *Abz2p* is the founder member of a new group of fungal 4-amino-4-deoxychorismate lyases that have no significant homology to its bacterial or plant counterparts. *Abz2p* appeared to form homodimers and dimerization was indispensable for its catalytic activity.

Tetrahydrofolate (vitamin B₉) and its folate derivatives are essential cofactors in all organisms and play a central role in one-carbon metabolism (2, 6). In their reduced form, folates act as the major cellular donors of one-carbon units in reactions involved in the synthesis of a wide variety of essential compounds such as glycine, methionine, purines, thymidylate, pantothenic acid, and *N*-formylmethionyl-tRNA (2). Folate deficiency provokes misincorporation of uracil into the DNA and chromosome breaks during the repair by uracil-DNA glycosylase and apyrimidinic endonuclease (7). Moreover, low-folate diets are associated with increased risk of developing cancer, and neural tube defects can be prevented by folic acid supplementation in early pregnancy (16).

Whereas most prokaryotes, microbial eukaryotes, and plants are able to biosynthesize folate *de novo*, mammals have lost this capacity, and they therefore rely on its dietary ingestion to meet their metabolic needs. Accordingly, mammals have evolved highly sophisticated uptake processes for transporting folates into cells, the reduced folate carrier being the primary route for the entry of reduced folates (28). The absence in mammals of a folate biosynthetic pathway has provided the basis for the development of antifolate sulfa drugs such as sulfonamides and sulfones, which deplete pathogenic microbial cells of essential growth folate (38).

The study of the folate biosynthetic pathway has been restricted to a few species of bacteria and plants (4, 5, 15). The folate molecule is tripartite, comprising of pteridine, glutamate, and *p*-aminobenzoate (PABA) moieties. In *Escherichia coli*, folic acid is biosynthesized by coupling of PABA and 7,8-dihydro-6-hydroxymethylpterin pyrophosphate to produce 7,8-dihydropteroate, which is subsequently glutamylated to give 7,8-dihydrofolate and reduced to yield tetrahydrofolate. The PABA moiety is synthesized in two steps catalyzed by two separate enzymes (Fig. 1). In bacteria, aminodeoxychorismate synthase (a heterodimeric enzyme formed by the association of the subunits encoded in *E. coli* by *pabA* and *pabB*) synthesizes 4-amino-4-deoxychorismate (ADC) from chorismate and glutamine (15). However, the pathway leading to PABA in *Saccharomyces cerevisiae* has not yet been completely elucidated. A bifunctional gene (*ABZ1*) encodes a protein bearing similarity to the two components (PabA and PabB) of ADC synthase described for *E. coli* (9). However, the gene that presumably encodes ADC lyase in yeast remains to be identified. Based on a large-scale screening of yeast mutants hypersensitive to the toxic PABA-analogue sulfanilamide, we identified a gene of previously unknown function (*YMR289w/ABZ2*) that is required for the biosynthesis of PABA. Here we show that the enzyme encoded by *ABZ2* is needed to convert ADC to PABA. On the basis of sequence similarity, the product of *ABZ2* is representative of a group of relatively homologous ADC lyases from fungi that are distantly related to the prokaryotic and plant enzymes. This finding completes the identification of the 10 enzymatic steps that convert PABA and GTP into tetrahydrofolate in the pathway for vitamin B₉ biosynthesis in yeast.

* Corresponding author. Mailing address: Departamento de Microbiología y Genética, Instituto de Microbiología Bioquímica, Universidad de Salamanca/CSIC, Campus Miguel de Unamuno, 37007 Salamanca, Spain. Phone: 34 923 294671. Fax: 34 923 224876. E-mail: revuelta@usal.es.

[∇] Published ahead of print on 14 September 2007.

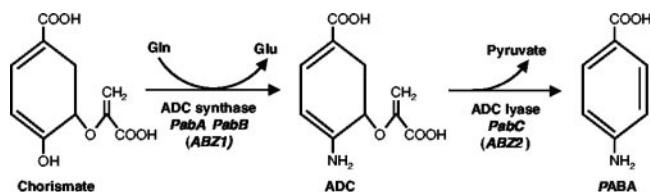


FIG. 1. Biosynthesis of PABA in *E. coli* and in *S. cerevisiae*. Names in italics show the *E. coli* genes that encode the enzyme. PabA and PabB associate to form the ADC synthase complex. Name in italics and in parentheses represents the corresponding *S. cerevisiae* gene; *ABZ1* encodes a bifunctional PabA-PabB ADC synthase. pABA, PABA.

MATERIALS AND METHODS

Yeast strains and growth conditions. The collection of nonessential haploid *MAT α* yeast deletion strains derived from parental strain BY4742 (*MAT α his3 Δ 1 leu2 Δ 0 lys2 Δ 0 ura3 Δ 0*) was obtained from Euroscarf (Frankfurt, Germany; <http://web.uni-frankfurt.de/fb15/mikro/euroscarf/index.html>), while the essential heterozygous diploids set was obtained from Invitrogen (catalog no. 95401.H5R3). The deletion strains were generated by the *Saccharomyces* Genome Deletion Project (http://www-sequence.stanford.edu/group/yeast_deletion_project/deletions3.html) by replacing the target gene with a kanamycin resistance cassette, *KanMX4*, by means of a PCR-based gene disruption strategy (44).

Yeast strains were grown on standard rich medium YPD (1% yeast extract, 2% Bacto peptone, 2% glucose) and synthetic minimal medium (SMM) (43) supplemented with the nutritional requirements of the parental strain. Agar (2%) was added for solid plates. All yeast cultures were incubated at 28°C.

Large-scale sulfanilamide sensitivity screenings. Approximately 4,800 haploid deletion strains in the BY4742 background and 1,100 heterozygous essential diploids were screened for hypersensitivity to sulfanilamide in liquid SMM. The strains were pinned from 96-well frozen stock plates by using a stainless steel 96-pin replicator (Nalgene Nunc International) into 96-well plates containing 150 μ l of liquid YPD medium supplemented with G418 (150 μ g/ml; Gibco-BRL). Several replicates of the corresponding wild-type strain were included in the master plates to minimize experimental noise due to intra- and interexperimental variations. The plates were incubated at 28°C for 3 days and then pin-replicated onto liquid SMM 96-well plates containing either no drug or 200 μ g of sulfanilamide (Sigma)/ml. Plates were incubated at 28°C, and growth was scored quantitatively every 24 h over a period of 5 days by obtaining readings of the optical density at 595 nm, using a microplate reader spectrophotometer (model 550; Bio-Rad Laboratories). Putative sulfanilamide-hypersensitive strains identified during the screening of the yeast knockout collection were further retested at least in duplicate under the same conditions described for the screenings. Strains with enhanced sensitivity to sulfanilamide were selected based on a growth inhibition (GI), after 96 h of sulfanilamide treatment, of >75%. The GI was calculated according to the following equation: $GI = 100 \times [(growth\ of\ mutant\ in\ control\ medium - growth\ of\ mutant\ in\ drug-containing\ medium) / growth\ of\ mutant\ in\ control\ medium]$.

Functional complementation assays. For complementation assay of the *E. coli* PabC function, a *pabC* deletion mutant was constructed in the *E. coli* strain BW25113 background according to published procedures (8). Briefly, a *pabC* deletion cassette was constructed by using the N-terminal *pabC* deletion primer (5'-CCGTAGTGAACATGCTGCCACACTAACAATTCTCTGATAAAGGAGCCGGTCCGATCCCCGGGTAATTA-3') and the C-terminal *pabC* deletion primer (5'-CCCAGTACCACAGCAATAACAAGATTATCAATAAACAATTTCATGATGAATTCGAGCTCGTTTAA-3') to amplify the *loxP*-*kanMX-loxP* module that confers kanamycin resistance in *E. coli* (17). The deletion primers were designed to contain 49-nucleotide homology extensions and 19-nucleotide priming sequences for pUG6 as a template. The ~1,500-bp PCR product was purified and then electrotransformed into *E. coli* strain BW25113 carrying the λ Red expression plasmid pJJ790 (19). After primary selection on medium containing kanamycin (50 μ g/ml), mutants were maintained on medium without antibiotic. They were colony-purified once nonselectively at 37°C and then checked for chloramphenicol sensitivity (25 μ g/ml) to test for the loss of the helper pJJ790 plasmid. A number of kanamycin-resistant, chloramphenicol-sensitive transformants were also found to be PABA auxotrophs. One of them, JR3125 ($\Delta pabC$), was selected and confirmed by analytical PCR and sequencing to carry the desired deletion.

E. coli JR3125 ($\Delta pabC$) was transformed with YEpl352 (20) or a YEpl352-

based plasmid containing an insert spanning the complete *ABZ2* coding sequence and 329 and 441 bp of the upstream and downstream regions, respectively. Complementation growth tests were done by culture at 37°C in liquid M9 minimal medium containing 50 μ g of kanamycin/ml and 100 μ g of ampicillin/ml, with or without 200 ng of PABA/ml, and measuring the absorbance at different time intervals.

Expression and purification of Abz2p. To express the full-length Abz2 protein, a plasmid was generated by inserting the *S. cerevisiae* *ABZ2* coding sequence (PCR amplified) between the NdeI and BamHI cloning sites of the pET-28b expression plasmid (Novagen). In the recombinant vector (pET28b-Abz2), the Abz2 polypeptide is fused in frame with an N-terminal peptide containing six tandem histidine residues, and expression of the His-tagged protein is driven by a T7 RNA polymerase promoter. The DNA sequence of the insert was confirmed.

The pET28b-Abz2 recombinant plasmid was transformed into *E. coli* BL21(DE3), and a 1,000-ml culture of *E. coli* BL21(DE3)/pET28b-Abz2 was grown at 37°C in Luria-Bertani medium containing 50 μ M pyridoxal phosphate and 30 μ g of kanamycin/ml until achieving an A_{600} of 0.8. The culture was adjusted to 0.4 mM IPTG (isopropyl- β -D-thiogalactopyranoside), and incubation was continued at 18°C for 20 h. The cells were then harvested by centrifugation, and the pellet was stored at -80°C. All subsequent procedures were performed at 4°C. Thawed bacterial pellets were resuspended in 50 ml of lysis buffer A (50 mM potassium phosphate buffer [pH 7.5], 500 mM NaCl, 20 mM imidazole, 0.01 M β -mercaptoethanol, protease inhibitor cocktail [Roche Diagnostics]), and cell lysis was achieved by the addition of 1 mg of lysozyme/ml. The lysates were sonicated to reduce viscosity, and any insoluble material was removed by centrifugation at 15,000 \times g for 45 min.

The soluble extract was applied to a 5-ml Ni-affinity column (HisTrap HP; GE Healthcare) that had been equilibrated with buffer A. The column was washed with the same buffer and then eluted stepwise with the same buffer containing 50, 100, 200, 300, 400, or 500 mM imidazole. The recombinant Abz2 polypeptide was retained in the column and was recovered mainly in the 300 mM imidazole eluate. After desalting on a PD-10 column (GE Healthcare) the eluate was loaded onto a 5-ml MonoQ HR 5/5 column (0.5 \times 5-cm HR 5/5, \AA KTA FPLC System; GE Healthcare), which was equilibrated with buffer B (50 mM potassium phosphate buffer [pH 7.5], 50 mM NaCl, 0.01 M β -mercaptoethanol). The column was then washed with 5 ml of the same buffer, and the chromatography was developed with a 25-ml linear gradient 50 to 500 mM NaCl in buffer B. Fractions from MonoQ chromatographies containing apparently pure Abz2p were pooled and desalted on a PD-10 column, and glycerol was added (10% [vol/vol] final concentration) prior to storage at -80°C. The purity of the protein was checked by sodium dodecyl sulfate-polyacrylamide gel electrophoresis (SDS-PAGE) (26). The protein concentration was determined by the Bio-Rad dye binding method, using bovine serum albumin as standard (Bio-Rad).

Enzyme assays. Stock solutions (5 mM) of chorismic acid (Sigma) were extracted three times with diethyl ether to remove contaminating 4-hydroxybenzoate. L-Glutamine and PABA, obtained from Sigma, were used without any additional purification. ADC lyase activity was determined as described previously with minor modifications (14). Standard glutamine-dependent assays designed to generate the intermediate ADC contained 50 mM Tris-HCl (pH 7.5), 5 mM MgCl_2 , 10 mM dithiothreitol, 200 mM chorismate, 5 mM L-glutamine, 3% glycerol, and 15 μ g of recombinant yeast PABA synthase (provided by E. Fernandez, Universidad de Salamanca, Spain) and were incubated at 30°C for 2 h with total conversion of chorismate into ADC. At this time, 15 μ g of purified recombinant Abz2p protein was added, and the reaction mixture was incubated at the same temperature. At different times, samples (100 μ l) were removed; the reactions were stopped with 20 ml of 75% acetic acid, incubated on ice for 1 h, and centrifuged (15,000 \times g, 4°C, 15 min). Reaction controls lacking PABA synthase, Abz2p, or both proteins were also performed. The supernatant was separated isocratically on a 250-by-4.6-mm C_{18} reverse-phase column (Bio-Sil C18 HL 90-5 S; Bio-Rad) with 5% (vol/vol) acetic acid as the mobile phase, and the elution of chorismate, ADC, and PABA was monitored at 280 nm. The reaction products were identified and quantified by their UV absorption spectra (30) and elution times relative to standards.

Molecular mass determination. The apparent native molecular mass of purified yeast recombinant ADC lyase was determined via blue native gel electrophoresis and gel filtration chromatography. Gel filtration chromatography was performed on a Superdex 200 HR 10/30 GL column (\AA KTA System; GE Healthcare) calibrated with a MWGF200 kit for molecular weights from Sigma. Blue native gel electrophoresis was done as previously described (39) on a 4 to 16% polyacrylamide gradient gel (NativePAGE Novex; Invitrogen). For blue native gel electrophoresis NativeMark unstained protein standards (Invitrogen) were used. The method of Laemmli (26) was used for SDS-PAGE determination of

TABLE 1. Functional classification of genes whose deletion causes hypersensitivity to sulfanilamide

Function	No. of genes	Mutants hypersensitive to sulfanilamide ^a
One-carbon metabolism	17	<i>ABZ1</i> , <i>ADK1</i> , <i>ADE6</i> , <i>ARO1</i> , <i>CKB1</i> , <i>CKB2</i> , <i>FOL2*</i> , <i>GSH1</i> , <i>GUK1</i> , <i>HRT1</i> , <i>MET6</i> , <i>MET18</i> , <i>MET28</i> , <i>MET30</i> , <i>PHO2</i> , <i>RIB3</i> , <i>TRM7</i>
Amino acid metabolism	8	<i>BRO1</i> , <i>CCR4</i> , <i>LST8</i> , <i>NOT5</i> , <i>PTR3</i> , <i>RTG1</i> , <i>TRP5</i> , <i>URE2</i>
Lipid metabolism	16	<i>ARG82</i> , <i>DEP1</i> , <i>ERG4</i> , <i>ERG6</i> , <i>ERG28</i> , <i>FAB1</i> , <i>GPII</i> , <i>HEM14</i> , <i>MVD1</i> , <i>NSG2</i> , <i>OPI1</i> , <i>PHO23</i> , <i>RXT2</i> , <i>SAP30</i> , <i>UME6</i> , <i>VPS34</i>
Vacuole and vesicular transport	24	<i>CHC1</i> , <i>PEP3</i> , <i>PEP5</i> , <i>RGPI</i> , <i>SEC12</i> , <i>SLA2</i> , <i>TFP1</i> , <i>TFP3</i> , <i>TSA1</i> , <i>VMA4</i> , <i>VMA5</i> , <i>VMA7</i> , <i>VMA8</i> , <i>VMA10</i> , <i>VMA13</i> , <i>VMA16</i> , <i>VMA21</i> , <i>VMA22</i> , <i>VPH2</i> , <i>VPS16</i> , <i>VPS45</i> , <i>VPS52</i> , <i>VPS54</i> , <i>VRP1</i>
DNA metabolism and cell cycle	28	<i>ARP5</i> , <i>ARP8</i> , <i>CAK1</i> , <i>CDC2</i> , <i>CDC8</i> , <i>FUR4</i> , <i>FYV6</i> , <i>GCN5</i> , <i>GRR1</i> , <i>HYS2</i> , <i>INO80</i> , <i>IRRI</i> , <i>KEM1</i> , <i>MCD1</i> , <i>POL32</i> , <i>RAD52</i> , <i>RFC2</i> , <i>RNR2</i> , <i>RRM3</i> , <i>RSC6</i> , <i>RTT109</i> , <i>SGF29</i> , <i>SNF2</i> , <i>SPC72</i> , <i>SPT3</i> , <i>STH1</i> , <i>SWD1</i> , <i>YRB1</i>
Biological process unknown	6	<i>OPI9</i> , <i>YBL100C</i> , <i>YCL007C</i> , <i>YHI9</i> , <i>YMR289W</i> , <i>YOR331C</i>
Other functions	18	
Carbohydrate metabolism		<i>BCY1</i> , <i>SGA1</i> , <i>SHP1</i> , <i>TPS2</i>
Mannosylation		<i>ANP1</i> , <i>KRE2</i> , <i>MNN9</i> , <i>OCH1</i>
Transcription		<i>HPR1</i> , <i>RLR1</i> , <i>RPB4</i> , <i>SNF4</i> , <i>SUB1</i> , <i>THP1</i> , <i>TUP1</i>
Energy		<i>AAC3</i> , <i>ATP1</i> , <i>ATP2</i>

^a Genes identified among the essential heterozygous diploids set are indicated in boldface.

the molecular mass of the Abz2 polypeptide under denaturing conditions. Identification of proteins by tryptic peptide mass fingerprinting (done by the Servicio de Proteómica, CIC, Salamanca, Spain) was performed as described previously (24).

Computational methods. Similarity searches were performed using BLAST software (1) at the National Center for Biotechnology Information (www.ncbi.nlm.nih.gov). Protein domains or motifs were searched for in Abz2 using the InterProScan program and the InterPro database of protein families at the European Bioinformatics Institute (www.ebi.ac.uk). Multiple sequence alignments were done with CLUSTAL W (41), using the European Bioinformatics Institute tools (www.ebi.ac.uk). Molecular phylogenetic analysis was carried out by using MEGA v 3.1 software (22).

RESULTS

Genome-wide screening for sulfanilamide-hypersensitive mutants. Using the collection of yeast haploid knockout strains and the heterozygous essential diploids set, we performed a chemical genomic screening to identify the spectrum of genes whose deletion alters the fitness profile in the presence of the PABA antimetabolite sulfanilamide. Although the majority of the deletion strains grown grew comparably to wild-type cells on SMM supplemented with sulfanilamide (200 µg/ml), a large number of mutant strains showed mild growth retardation (data not shown). At least 117 strains, however, showed a severe growth defect (75% GI) caused by the presence of the antifolate drug in the medium. Functional classification of the hypersensitive mutants revealed that they were affected in different biological processes, including those involved in vacuole and vesicular transport, DNA metabolic and cell cycle processes, lipid and amino acid metabolism, and others of unknown function (Table 1), indicating that different aspects of their cellular biology were compromised by sulfanilamide treatment. As expected, one group of mutants was related to folate and one-carbon metabolism and encompassed genes involved in the regulation of, or with a direct catalytic role in, the biosynthesis of folates, purine and pyrimidine nucleotides, sulfur, and one-carbon metabolism. Moreover, *ABZ1*, the one previously known member of the PABA biosynthetic pathway, was recovered, thus validating our screening. In addition, we found that the deletion of six genes of uncharacterized

function also caused sensitivity to sulfanilamide. Four of them were dubious open reading frames (ORFs)—*OPI9*, *YBL100c*, *YCL007c*, and *YOR331c*—that overlapped verified genes also found to be hypersensitive in our sulfanilamide screening, thus validating this assay. The other two genes (*YHI9* and *YMR289w*) likely encode proteins although their function remains unknown.

Identification of *YMR289W* as the *ABZ2* gene. In the present study we focused on *YMR289w*. Further characterization of the *ymr289w* mutant revealed a slow growth on SMM, a phenotype that resulted in the inability to grow after two successive subcultures in the same medium. This suggests that the *ymr289w* mutant strain is impaired in the synthesis of an essential metabolite whose cellular pool is exhausted after prolonged culture. The hypersensitivity to the antifolate sulfanilamide displayed by *ymr289w* cells points to the folic acid biosynthetic pathway as being responsible for the auxotrophy of the mutant. This hypothesis was confirmed by the fact that the addition of folic acid (2 µg/liter) to the minimal medium restored the ability of the mutant to grow (Fig. 2). Supplementation of the minimal medium with PABA (200 ng/ml) also rescued the growth defect of the mutant cells, indicating that the *YMR289w* gene (named *ABZ2* according to the yeast gene nomenclature guidelines) is involved in the biosynthesis of this folic acid precursor. A YEp352-derived multicopy plasmid harboring the cognate *YMR289w* gene also rendered the *ymr289w* (*abz2*) mutant able to grow in a minimal medium lacking PABA or folic acid, thus demonstrating that no mutation other than the deletion of the *ABZ2* (*YMR289w*) gene was responsible for the PABA auxotrophy.

***ABZ2* functionally complements an *E. coli* *pabC* mutant.** The synthesis of PABA in *E. coli* is carried out by three enzymes encoded by the genes designated *pabA*, *pabB*, and *pabC*. In yeast, an ADC synthase gene (*ABZ1*) has been described that encodes a bifunctional protein containing the two domains homologous to the two components—PabA and PabB—of the prokaryotic ADC synthase (9). The identification in *S. cerevisiae* of a second gene, *ABZ2*, involved in the biosynthesis

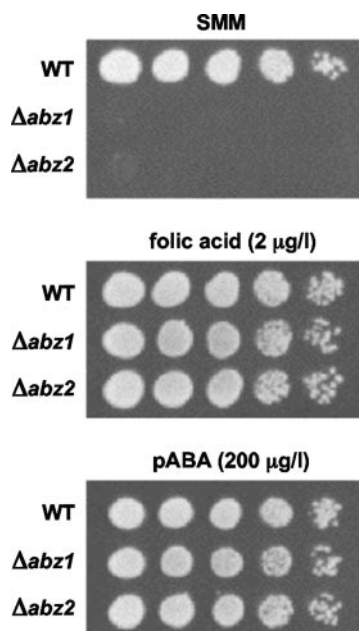


FIG. 2. Folic acid and PABA restore growth of *S. cerevisiae* $\Delta abz1$ and $\Delta abz2$ ($\Delta ymr289w$) mutant strains. BY4742 (wild-type) and $\Delta abz1$ and $\Delta abz2$ mutant strains were grown in SMM. After two successive subcultures in SMM consisting of a 100-fold dilution of a late-exponential-phase culture and allowed to reach late-exponential-phase, samples of the cultures were diluted, spotted onto solid SMM supplemented with folic acid or PABA at the indicated concentrations, and examined for growth after incubation at 28°C for 5 days.

PABA suggests that this gene is functionally homologous to the bacterial *pabC* gene.

To check that *ABZ2* was able to complement the deficiency of the *pabC* function, we constructed an *E. coli pabC* single-gene mutant by the PCR-based inactivation method as described in Materials and Methods (8). One $\Delta pabC$ mutant, designated JR3125, was verified by PCR amplification and sequencing and was selected for the complementation assays.

The deletion of the *pabC* gene in the JR3125 strain resulted in a severe impairment of growth in M9 minimal medium that could be rescued by the addition of PABA (200 ng/ml) to the medium (Fig. 3). The transformation of JR3125 with a YEp352-derived vector containing the complete *ABZ2* ORF and 329 and 441 bp of the upstream and downstream regions, respectively, was also able to restore the ability to grow in the absence of PABA up to nearly the wild-type rate of growth (Fig. 3). However, no complementation was seen in the *pabC* deletion mutant transformed with the empty vector. These results show that the *ABZ2* gene is the yeast functional homologue of the prokaryotic *pabC* gene.

Recombinant Abz2p has ADC lyase activity. The complementation assay and the sequence analyses suggested that *ABZ2* encodes an ADC lyase in yeast. A direct test of the hypothesis that Abz2p catalyzes the β -elimination of pyruvate and aromatization of the ADC to give PABA required the preparation of the pure polypeptide. Since Abz2p is a scarce protein in yeast (11), the Abz2 polypeptide was overexpressed in *E. coli* as a fusion protein containing an N-terminal His₆ tag. The N-terminal extension did not interfere with activity, since

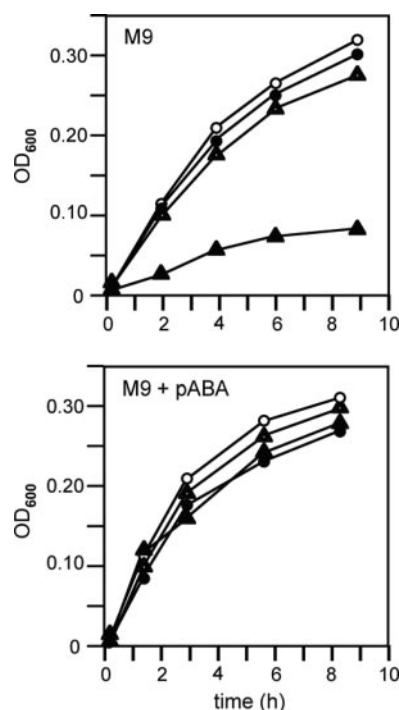


FIG. 3. Yeast *ABZ2* complements an *E. coli pabC* mutant. *E. coli* BW25113 wild-type (*pabC*) cells transformed with the empty plasmid YEp352 (●) or YEp352-*ABZ2* (○) and JR3125 ($\Delta pabC$) mutant cells transformed with the empty plasmid YEp352 (▲) or YEp352-*ABZ2* (△) were inoculated into M9 liquid medium containing 100 μg of ampicillin/ml and the absence or presence of 200 ng of PABA/ml. The cultures were incubated with aeration at 37°C and growth was recorded by measuring the absorbance at 600 nm.

the expression of this fusion protein in the *E. coli* $\Delta pabC$ mutant restored growth on M9 medium lacking PABA and resulted in a 50-fold increase in ADC lyase activity in *E. coli* whole-cell extracts (not shown). The Abz2p recombinant protein was purified as described in Materials and Methods and used in *in vitro* ADC lyase assays. Because the 4-amino-4-deoxychorismate substrate was not commercially available, we prepared it enzymatically from chorismate and glutamine using recombinant ADC synthase from yeast in a coupled assay. ADC synthase, the product of *ABZ1*, catalyzes the synthesis of 4-amino-4-deoxychorismate by replacing the hydroxyl group of chorismate with an amino group acid supplied by glutamine (9).

The substrate chorismate, the intermediate ADC, and the final product PABA all absorb at 280 nm but can be readily separated by reversed-phase high-pressure liquid chromatography (HPLC). We confirmed this chromatographic separation with elution times comparable to that reported previously (14). Therefore, after HPLC separation it is possible to determine the conversion of chorismate to ADC due to the enzymatic action of Abz1p; subsequent addition of ADC lyase to the reaction mixture can be used to analyze the conversion of the ADC intermediate to PABA. Addition to the reaction mixture of purified Abz1p led to a decrease in chorismate and the concomitant formation of ADC. After 2 h of incubation almost a total conversion of chorismate into ADC was achieved (Fig. 4). At this time, purified Abz2p protein was added to the reaction

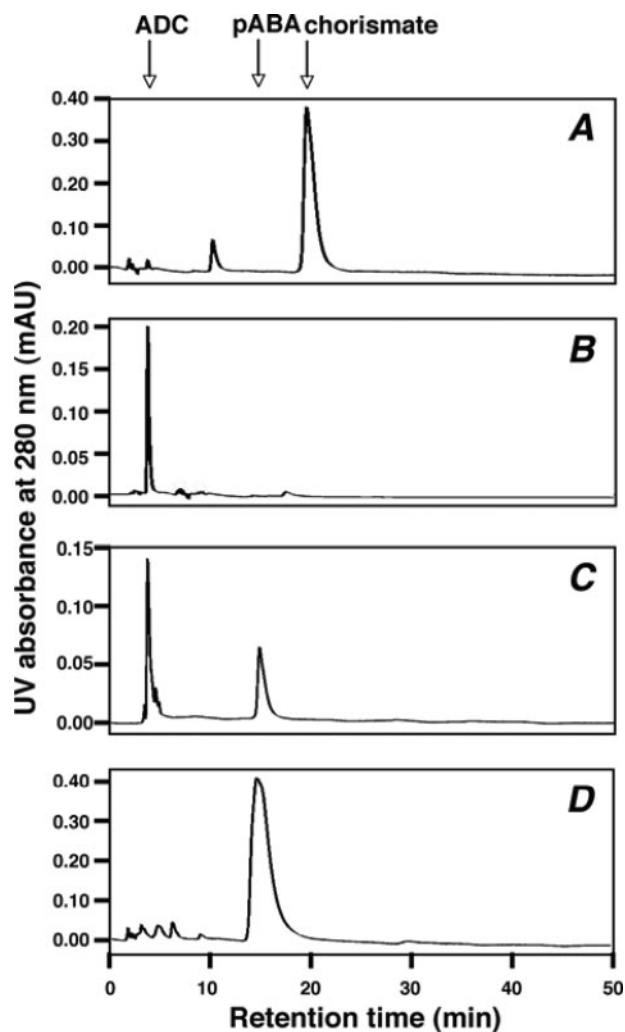


FIG. 4. Enzymatic conversion of ADC into PABA by recombinant yeast Abz2p. Representative HPLC elution profiles for extracts of incubation mixtures consisting of 50 mM Tris-HCl (pH 7.5), 5 mM MgCl₂, 10 mM dithiothreitol, 3% glycerol, 200 mM chorismate, and 5 mM L-glutamine. Reactions were initiated with the addition of 15 μ g of recombinant yeast Abz1p and incubated at 30°C for 2 h to allow the conversion of chorismate into ADC. At several times samples (100 μ l) were removed and analyzed by reversed-phase HPLC. The chromatograms shown correspond to the samples taken before the addition of the enzyme (A), and after 2 h of incubation (B). After 2 h, purified recombinant Abz2p (15 μ g) was added and incubation was then continued for 90 min at 30°C. PABA formation was monitored at different incubation times (C, 15 min; D, 90 min). The elution positions of chorismate, ADC and PABA are indicated with arrows. mAU, milli-absorbance unit.

mixture. The presence of Abz2p catalyzed the conversion of ADC into PABA in a time-dependent manner. Control reactions revealed that ADC synthase and ADC lyase enzymatic activities were dependent on the presence of Abz1 and Abz2 proteins, respectively (data not shown). Thus, these results show that *ABZ2* encodes a functional ADC lyase that catalyzes the last step in the synthesis of PABA of the folic acid pathway.

Dimeric structure of yeast ADC lyase. Most class IV amino acid aminotransferase-like pyridoxal phosphate-dependent enzymes are homodimers (10). Moreover, the crystal structure of

E. coli ADC lyase has been recently determined and shown to form homodimers (29). The subunit composition of Abz2p was analyzed by using blue native gel electrophoresis. Apparently pure recombinant Abz2p was applied to a 4 to 16% gradient blue native gel (Fig. 5A). Two dominant forms could be identified with approximate molecular masses of 50 and 100 kDa. The estimated molecular mass of the smaller form corresponded well to that of the monomeric Abz2 polypeptide, as calculated from its amino acid sequence and demonstrated by SDS-PAGE electrophoresis analysis (45 kDa) (Fig. 5A). The larger and slightly less abundant one apparently represents the Abz2p homodimer. The identity of both complexes was confirmed by tryptic peptide mass fingerprinting (data not shown).

The dimeric state of Abz2p was also investigated by analytical size exclusion chromatography on a Superdex 200 column calibrated with soluble proteins. The recombinant Abz2p preparation eluted in two distinct peaks, with apparent molecular masses of 45 and 92 kDa, in agreement with the sizes expected for the monomeric and homodimeric forms of Abz2p, respectively (Fig. 5B). ADC lyase activity analyses of the eluted fractions revealed that only fractions containing the dimeric Abz2p were enzymatically active, indicating that dimerization is indispensable for catalytic activity (Fig. 5B).

Fungal ADC lyases are distantly related to prokaryotic and plant ADC lyases. A BLASTp search of the whole GenBank database with the deduced protein product of *ABZ2* detected as the closest homologues a group of proteins of unknown function belonging to different fungal species. These proteins show sufficient homology to Abz2p (identity percentages ranging from 37% for *Ashbya gossypii* to 26% for *Neurospora crassa*) to predict that they represent authentic ADC lyases in those fungal species (Fig. 6A). Strikingly, specialized BLAST searches with Abz2p restricted to the bacterial or plant entries of the GenBank database failed to detect homologues, although experimentally characterized ADC lyases have been described in *E. coli*, tomato, and *Arabidopsis thaliana*. Phylogenetic analysis of representative ADC lyase sequences confirmed that the fungal ADC lyase group clustered well apart from the bacterial and plant ADC lyase groups, although clearly belonging to an ADC lyase subfamily of proteins that is divergent from the structurally related branched-chain amino acid aminotransferase family (Fig. 6B). In fact, a search of the InterPro database (36) for domains or protein motifs present in Abz2p revealed the presence of a domain characteristic of the amino acid aminotransferase-like pyridoxal phosphate-dependent enzymes. In addition to ADC lyases, this superfamily of proteins also encompasses branched-chain amino acid aminotransferases and prokaryotic D-aminotransferases, which are characterized by the presence of a pyridoxal phosphate-binding site located at the interface of a large and a small domain linked by a flexible loop (29). Important residues that are believed to be catalytically essential in ADC lyases are all conserved in Abz2p, as well as in the fungal homologues analyzed in the present study (Fig. 6A).

DISCUSSION

Despite the overwhelming impact of systematic genome sequencing on the understanding of the biology and evolution of organisms, enormous gaps remain in our current knowledge of

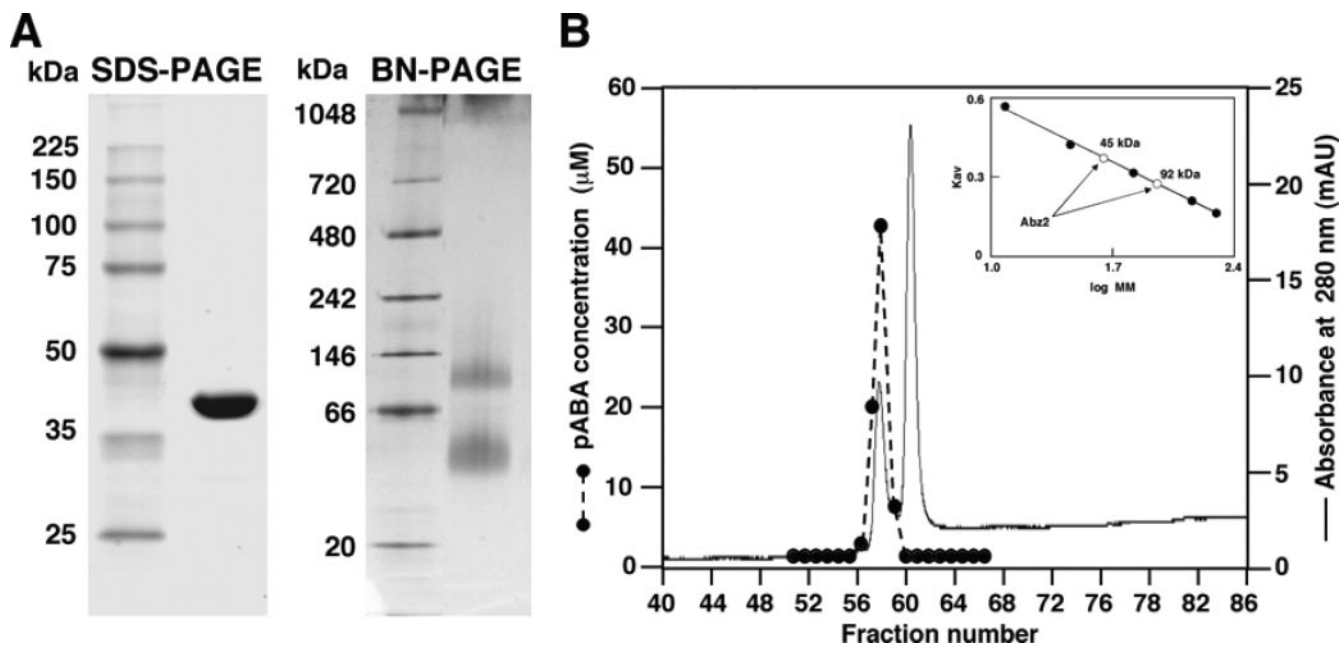


FIG. 5. Dimeric structure of the Abz2 protein. (A) SDS-PAGE and blue native gel electrophoresis (BN-PAGE) analyses of the purified recombinant Abz2p. Samples ($\sim 5 \mu\text{g}$) of purified recombinant Abz2p were loaded on a SDS-14% PAGE gel or on a 4 to 16% gradient blue native gel along with appropriate molecular mass markers. The calculated values for the monomeric and dimeric forms of Abz2p were about 50 and 100 kDa, respectively. (B) Gel filtration chromatography of Abz2p. The protein, 4 to 8 mg of purified recombinant Abz2p, was eluted with 50 mM Tris-HCl buffer (pH 7.5) through a Superdex 200 HR 10/30 column calibrated with molecular mass markers (cytochrome *c*, horse heart, 12.4 kDa; carbonic anhydrase, bovine erythrocytes, 29 kDa; albumin, bovine serum, 66 kDa; alcohol dehydrogenase, yeast, 150 kDa; β -amylase, sweet potato, 200 kDa). Fractions were assayed for protein concentration (absorbance at 280 nm) and for PABA synthesis from chorismate (200 mM) and L-glutamine (5 mM) in the presence of an excess of yeast ADC synthase protein. The inset shows the column calibration fitting the plot of the elution volume versus the logarithm of the molecular weight of the markers. The apparent molecular masses (MM) of the monomeric and dimeric forms of Abz2p were determined to be approximately 45 and 92 kDa, respectively.

the function of in silico-defined genes. For instance, in spite of being one of the best-known and most-studied eukaryotic model systems, ca. 21% of *S. cerevisiae* protein sequences still cannot be assigned a precise function. Awareness of this issue has permeated the yeast biology community and presents an important challenge (35).

Large-scale analyses have proved to be useful tools in providing functional clues to the set of still uncharacterized genes (3). In particular, chemical genetic profiling, which simultaneously probes the sensitivity of all deletion strains to a small molecule—often a metabolic inhibitor—has the advantage of inherently revealing phenotypes (12, 33). Here we performed a chemical genomic screening to identify the spectrum of genes whose deletion alters the fitness profile in the presence of the PABA antimetabolite sulfanilamide, both in the yeast nonessential haploid and in essential heterozygous sets. Essential heterozygous gene deletion mutants showing increased sensitivity to a drug might represent genes whose products are direct drug targets, genes that exhibit synthetic interactions with the drug target and that are upstream or downstream in the therapeutically relevant pathway, or genes encoding proteins involved in the transport or metabolism of the drug.

Although a detailed analysis of all of the functional categories disturbed by sulfanilamide is beyond of the scope of the present study, it is worth noting that in our screening we were able to identify a significant number of genes involved in folate/one-carbon metabolism. The sublethal concentration of the

sulfa drug used in the screening probably competes with PABA and dihydrofolate (34), therefore reducing the pool of folate cofactors and affecting a variety of biosynthetic pathways dependent on one-carbon transfer, including the synthesis of purines, thymidylate, *N*-formylmethionyl-tRNA, and some amino acids. Indeed, the screening identified a broad range of gene functions affected by sulfanilamide-induced cytotoxicity (Table 1). As expected, we found a significant number of mutants involved directly or indirectly in one-carbon/folate metabolism (*abz1*, *aro1*, and *fol2*), sulfur metabolism (*ckb1*, *ckb2*, *gsh1*, *hrt1*, *met6*, *met18*, *met28*, and *met30*), and nucleotide metabolism (*ade6*, *adk1*, *cdc8*, *guk1*, *pho2*, *rib3*, *rnr2*, and *trm7*), highlighting the validity of our experimental approach.

Folate pool depletion indirectly blocks dTMP production, leading to dTTP depletion, misincorporation of uracil into DNA during replication, and imbalance in deoxynucleoside triphosphate pools, ultimately causing DNA damage and cytotoxicity due to the so-called “thymineless death” (23, 25). Interestingly, the screening reproducibly yielded mutants lacking deoxynucleoside monophosphate kinase activities (*adk1*, *cdc8*, and *guk1*) or defective in other regulatory or enzymatic functions of nucleotide metabolism (*ade6*, *pho2*, and *rnr2*). This presumably reflects the detrimental effects of the nucleotide imbalance in the presence of the folate depletant agent. Moreover, DNA repair and DNA replication mutants (*fvy6*, *ino80*, *rad52*, *rfc2*, and *rmm3*, and DNA polymerase δ subunits *cdc2*, *hys2*, and *pol32*), as well as mutants involved in chromatin

modification (*arp5*, *arp8*, *gcn5*, *rsc6*, *rtt109*, *sgf20*, *snf2*, *spt3*, *sth1*, and *swd1*), are also severely compromised by the sulfa drug, as expected from the damaging cycles of uracil DNA misincorporation and attempted DNA repair of deoxyuridine residues.

We presume that the sulfonamide hypersensitivity of some mutants involved in cell homeostasis and vesicular transport is likely to be unspecific, since these mutants are affected in processes related to drug or stress responses and show pleiotropic defects in the presence of different insults (32, 45).

Several unexpected mutants involved in lipid metabolism and its regulation were also susceptible to sulfanilamide treatment. Of particular interest are the mutants affected in ergosterol biosynthesis, which—besides its role in membrane fluidity and permeability—have been linked to folate metabolism via *S*-adenosyl-L-methionine (31).

All of these observations reflect the complex phenotypes caused by sulfanilamide-mediated folate depletion, due directly to a one-carbon unit deficiency and indirectly affecting other processes, since many methylated molecules such as nucleic acids, proteins, and lipids are formed by transmethylation reactions with *S*-adenosyl-L-methionine. It is noteworthy that our findings could open new fields for exploring novel treatments for several bacterial, fungal, and protozoan infections because the combination of sulfa drugs with inhibitors of some of the sulfanilamide-compromised processes found could render these pathogens sensitive to combined therapy. Further research will be required to assess precisely how the genes identified influence the response to sulfanilamide treatment.

Among the genes whose deletion elicits sulfanilamide hypersensitivity, *YHI9* and *YMR289w* lack specific physiological functions. The three-dimensional crystal structure of Yhi9p has recently been determined, and it is classified as a member of the PhzF (PF02567) enzyme family that might use either chorismate or an anthranilate derivative as a substrate (27). No functional or structural data on *YMR289w* were available prior to this work.

Here we have demonstrated that the *YMR289w* ORF (*ABZ2* gene) of *S. cerevisiae* encodes an enzyme responsible for the last of the two steps in the PABA branch of the folate biosynthetic pathway. Heterologous complementation of an *E. coli* *pabC* mutation and direct enzymatic characterization of the Abz2 protein support this notion. Yeast *abz2* mutants impaired in the synthesis of PABA are able to grow on minimal medium supplemented either with PABA or with folic acid, indicating

that this metabolite does not have an essential function other than its role as a substrate in the synthesis of folates.

Yeast mutants deleted in *ABZ2* appear to be leaky for PABA auxotrophy. This characteristic, also observed in *E. coli* *pabC* mutants (13), has tacitly been attributed to the fact that ADC is unstable and is spontaneously converted to PABA in a nonenzymatic form (40). However, the apparent leakiness of the *abz2* mutants seems to be due to the existence in the cells of a PABA or a folate pool sufficient to support the growth and division of the cells for several generations. As described here, subculturing of the *abz2* mutant in medium lacking PABA or folate exacerbates its PABA auxotrophy, presumably because of the depletion of existing PABA or folate pools. In plants, most of the endogenous PABA content is not present as free acid but as a glucose ester (*p*-aminobenzoyl- β -D-glucopyranoside [PABA-Glc]). This conjugated PABA-Glc form is accumulated in the cytoplasm and has been proposed to serve as an accessible storage depot of PABA for use as a substrate to sustain the biosynthesis of folate that takes place in mitochondria (37). Although the formation of PABA-Glc has been not detected in yeast (37), it is likely that an equivalent storage form of PABA necessary to drive its transport to mitochondria would exist in this organism.

Although the analysis of *S. cerevisiae* ADC lyase revealed that the protein has no significant sequence homology to its bacterial or plant counterparts, the yeast enzyme does contain a domain typical of the class IV amino acid aminotransferases family (36). Furthermore, all of the residues proposed to be catalytically essential in *E. coli* ADC lyase (29) are also present in Abz2p (Fig. 6A). Thus, the conserved lysine residue that covalently binds pyridoxal phosphate can be found in position 251 in the yeast enzyme. Also present are residues Arg¹⁰⁷ and Glu²⁹⁷, which may directly interact with the enzyme and play a critical role in the catalytic function. Finally, the carboxylate groups of ADC could be recognized by Asn³⁶⁰ and Arg¹⁸², and the cyclohexadiene moiety could make van der Waals contact with the side chain of Leu³⁵⁸ (Fig. 6A).

Yeast ADC lyase appears to form dimers, a structural characteristic that is also shared by the *E. coli* and *A. thaliana* ADC lyases (5, 13, 29). Whereas the prokaryotic and plant enzymes have been detected only in their dimeric form, our analyses using blue native electrophoresis and size exclusion chromatography indicate that the dimeric form of the enzyme is in equilibrium with the monomeric form, although only the dimers are catalytically active. This equilibrium between active

FIG. 6. Comparison of *S. cerevisiae* ADC lyase to other fungal homologues and the experimentally characterized *E. coli* and *A. thaliana* ADC lyases. (A) Alignment of the deduced protein sequences from *S. cerevisiae* (S.c.; NP_014016), *A. gossypii* (A.g.; NP_986996), *Candida albicans* (C.a.; XP_715312), *Yarrowia lipolytica* (Y.l.; XP_502893), *Schizosaccharomyces pombe* (S.p.; NP_595968), *E. coli* (E.c.; A42954), and *A. thaliana* (A.t.; NP_200593). Conserved residues believed to be catalytically important according to the structure of *E. coli* ADC lyase (29) are boxed. (B) Molecular phylogenetic tree of inferred ADC lyase (ADCL) and structurally related branched-chain amino acid transaminase (BCAT) protein sequences from fungi, plants, and bacteria. The circled zone demarcates the fungal sequences. ADCL: Sc, *S. cerevisiae*; Ag, *A. gossypii*; Ca, *C. albicans*; Sp, *S. pombe*; Kl, *Kluyveromyces lactis* (XP_451419); Nc, *Neurospora crassa* (XP_961237); Ec, *E. coli*; Bs, *Bacillus subtilis* (NP_387957); At, *A. thaliana*; Le, *Lycopersicon esculentum* (AY547289). BCAT: BCAT1_Sc (NP_012078); BCAT2_Sc (NP_012682); BCAT_Ec (P00510); BCAT1_At (AAC34335); BCAT2_At (AAC34333); BCAT3_At (CAB66906); BACT5-At (BAB10685); BCAT6-At (AAF76437). The phylogenetic tree was constructed by using the neighbor-joining method of MEGA 3.1 (22). Each node was tested by using the bootstrap approach by taking 1,000 replications and a random seeding of 64,238 to ascertain the reliability of the nodes. The numbers indicated are in percentages against each node. Branch lengths were measured in terms of amino acid substitutions, with the scale indicated below the tree.

dimers and inactive monomers could be the basis of a mechanism of activity regulation of this enzyme, which does not appear to be feedback regulated for PABA or folates (5, 42), and neither does its expression seem to be subject to transcriptional control (our unpublished results). Although unlikely, the possibility still exists that the presence of Abz2p monomers in the enzyme preparation could be an artifact due to the presence of an N-terminal His₆ tag in the recombinant protein used in our analyses.

In contrast to plants, green fluorescent protein-tagged Abz2p is clearly located in the cytoplasm (results not shown), a finding in agreement with a previous report (21). Since Abz1p is also a cytoplasmic enzyme, it is clear that the synthesis of PABA in *S. cerevisiae* takes place in the cytoplasm and not inside an specific organelle, as occurs in the plastids of plants. In this respect, the presence of PABA freely distributed in the cytoplasm of fungi raises the issue of the possible existence of a specific PABA transporter in mitochondria where the tetrahydrofolate biosynthetic pathway must continue (18).

The identification in the present study of the last unknown gene involved in the biosynthesis of tetrahydrofolate in yeast enables the initiation of metabolic engineering projects aimed to the construction of valuable vitamin B₉ producer strains. In particular, overexpression of the PABA biosynthetic pathway could solve one of the major constraints of folate synthesis, namely, the supply of the PABA precursor.

ACKNOWLEDGMENTS

This study was supported by grants GEN2001-4707-C08-01 and AGL2005-07245-C03-03 from the Ministerio de Educación y Ciencia (Spain). J.B. and L.M. were supported by predoctoral fellowships from the Junta de Castilla y León and Universidad de Salamanca (Spain), respectively.

We thank M. D. Sánchez and M. M. Martín for excellent technical help and N. Skinner for correcting the manuscript.

REFERENCES

- Altschul, S. F., T. L. Madden, A. A. Schaffer, J. Zhang, Z. Zhang, W. Miller, and D. J. Lipman. 1997. Gapped BLAST and PSI-BLAST: a new generation of protein database search programs. *Nucleic Acids Res.* **25**:3389–3402.
- Appling, D. R. 1991. Compartmentation of folate-mediated one-carbon metabolism in eukaryotes. *FASEB J.* **5**:2645–2651.
- Bader, G. D., A. Heilbut, B. Andrews, M. Tyers, T. Hughes, and C. Boone. 2003. Functional genomics and proteomics: charting a multidimensional map of the yeast cell. *Trends Cell Biol.* **13**:344–356.
- Basset, G. J., E. P. Quinlivan, S. Ravel, F. Rebeille, B. P. Nichols, K. Shinozaki, M. Seki, L. C. Adams-Phillips, J. J. Giovannoni, J. F. Gregory III, and A. D. Hanson. 2004. Folate synthesis in plants: the *p*-aminobenzoate branch is initiated by a bifunctional PabA-PabB protein that is targeted to plastids. *Proc. Natl. Acad. Sci. USA* **101**:1496–1501.
- Basset, G. J., S. Ravel, E. P. Quinlivan, R. White, J. J. Giovannoni, F. Rebeille, B. P. Nichols, K. Shinozaki, M. Seki, J. F. Gregory III, and A. D. Hanson. 2004. Folate synthesis in plants: the last step of the *p*-aminobenzoate branch is catalyzed by a plastidial aminodeoxychorismate lyase. *Plant J.* **40**:453–461.
- Blakley, R. L., and S. J. Benkovic. 1984. Folates and pterins: chemistry and biochemistry of folates, vol. 1. John Wiley & Sons, Inc., New York, NY.
- Blount, B. C., M. M. Mack, C. M. Wehr, J. T. MacGregor, R. A. Hiatt, G. Wang, S. N. Wickramasinghe, R. B. Everson, and B. N. Ames. 1997. Folate deficiency causes uracil misincorporation into human DNA and chromosome breakage: implications for cancer and neuronal damage. *Proc. Natl. Acad. Sci. USA* **94**:3290–3295.
- Datsenko, K. A., and B. L. Wanner. 2000. One-step inactivation of chromosomal genes in *Escherichia coli* K-12 using PCR products. *Proc. Natl. Acad. Sci. USA* **97**:6640–6645.
- Edman, J. C., A. L. Goldstein, and J. G. Erbe. 1993. Para-aminobenzoate synthase gene of *Saccharomyces cerevisiae* encodes a bifunctional enzyme. *Yeast* **9**:669–675.
- Eliot, A. C., and J. F. Kirsch. 2004. Pyridoxal phosphate enzymes: mechanistic, structural, and evolutionary considerations. *Annu. Rev. Biochem.* **73**:383–415.
- Ghaemmaghami, S., W. K. Huh, K. Bower, R. W. Howson, A. Belle, N. Dephoure, E. K. O'Shea, and J. S. Weissman. 2003. Global analysis of protein expression in yeast. *Nature* **425**:737–741.
- Giaever, G., A. M. Chu, L. Ni, C. Connelly, L. Riles, S. Veronneau, S. Dow, A. Lucau-Danila, K. Anderson, B. Andre, A. P. Arkin, A. Astromoff, M. El-Bakkoury, R. Bangham, R. Benito, S. Brachat, S. Campanaro, M. Curtiss, K. Davis, A. Deutschbauer, K. D. Entian, P. Flaherty, F. Foury, D. J. Garfinkel, M. Gerstein, D. Gotte, U. Guldener, J. H. Hegemann, S. Hempel, Z. Herman, D. F. Jaramillo, D. E. Kelly, S. L. Kelly, P. Kotter, D. LaBonte, D. C. Lamb, N. Lan, H. Liang, H. Liao, L. Liu, C. Luo, M. Lussier, R. Mao, P. Menard, S. L. Ooi, J. L. Revuelta, C. J. Roberts, M. Rose, P. Ross-Macdonald, B. Scherens, G. Schimmack, B. Shafer, D. D. Shoemaker, S. Sookhai-Mahadeo, R. K. Storms, J. N. Strathern, G. Valle, M. Voet, G. Volckaert, C. Y. Wang, T. R. Ward, J. Wilhelm, E. A. Winzeler, Y. Yang, G. Yen, E. Youngman, K. Yu, H. Bussey, J. D. Boeke, M. Snyder, P. Philippsen, R. W. Davis, and M. Johnston. 2002. Functional profiling of the *Saccharomyces cerevisiae* genome. *Nature* **418**:387–391.
- Green, J. M., W. K. Merkel, and B. P. Nichols. 1992. Characterization and sequence of *Escherichia coli* pabC, the gene encoding aminodeoxychorismate lyase, a pyridoxal phosphate-containing enzyme. *J. Bacteriol.* **174**:5317–5323.
- Green, J. M., and B. P. Nichols. 1991. *p*-Aminobenzoate biosynthesis in *Escherichia coli*: purification of aminodeoxychorismate lyase and cloning of pabC. *J. Biol. Chem.* **266**:12971–12975.
- Green, J. M., B. P. Nichols, and B. P. Matthews. 1996. Folate biosynthesis, reduction, and polyglutamylation, p. 665–673. In F. C. Neidhardt, R. Curtiss III, J. L. Ingraham, E. C. C. Lin, K. B. Low, B. Magasanik, W. S. Reznikoff, M. Riley, M. Schaechter, and H. E. Umbarger (ed.), *Escherichia coli* and *Salmonella*: cellular and molecular biology, 2nd ed. American Society for Microbiology, Washington, DC.
- Greene, N. D., and A. J. Copp. 1997. Inositol prevents folate-resistant neural tube defects in the mouse. *Nat. Med.* **3**:60–66.
- Guldener, U., S. Heck, T. Fielder, J. Beinhauer, and J. H. Hegemann. 1996. A new efficient gene disruption cassette for repeated use in budding yeast. *Nucleic Acids Res.* **24**:2519–2524.
- Guldener, U., G. J. Koehler, C. Haussmann, A. Bacher, J. Kricke, D. Becher, and J. H. Hegemann. 2004. Characterization of the *Saccharomyces cerevisiae* Foll1 protein: starvation for C1 carrier induces pseudohyphal growth. *Mol. Biol. Cell* **15**:3811–3828.
- Gust, B., G. L. Challis, K. Fowler, T. Kieser, and K. F. Chater. 2003. PCR-targeted *Streptomyces* gene replacement identifies a protein domain needed for biosynthesis of the sesquiterpene soil odor geosmin. *Proc. Natl. Acad. Sci. USA* **100**:1541–1546.
- Hill, J. E., A. M. Myers, T. J. Koerner, and A. Tzagoloff. 1986. Yeast/*Escherichia coli* shuttle vectors with multiple unique restriction sites. *Yeast* **2**:163–167.
- Huh, W. K., J. V. Falvo, L. C. Gerke, A. S. Carroll, R. W. Howson, J. S. Weissman, and E. K. O'Shea. 2003. Global analysis of protein localization in budding yeast. *Nature* **425**:686–691.
- Kumar, S., K. Tamura, and M. Nei. 2004. MEGA3: integrated software for molecular evolutionary genetics analysis and sequence alignment. *Brief Bioinform.* **5**:150–163.
- Kunz, B. A., S. E. Kohalmi, T. A. Kunkel, C. K. Mathews, E. M. McIntosh, and J. A. Reidy. 1994. International Commission for Protection Against Environmental Mutagens and Carcinogens. Deoxyribonucleoside triphosphate levels: a critical factor in the maintenance of genetic stability. *Mutat. Res.* **318**:1–64.
- Kussmann, M., and P. Roepstorff. 2000. Sample preparation techniques for peptides and proteins analyzed by MALDI-MS. *Methods Mol. Biol.* **146**:405–424.
- Ladner, R. D. 2001. The role of dUTPase and uracil-DNA repair in cancer chemotherapy. *Curr. Protein Pept. Sci.* **2**:361–370.
- Laemmli, U. K. 1970. Cleavage of structural proteins during the assembly of the head of bacteriophage T4. *Nature* **227**:680–685.
- Liger, D., S. Quevillon-Cheruel, I. Sorel, M. Bremang, K. Blondeau, I. Aoulfath, J. Janin, H. van Tilbeurgh, and N. Leulliot. 2005. Crystal structure of YHI9, the yeast member of the phenazine biosynthesis PhzF enzyme superfamily. *Proteins* **60**:778–786.
- Moscow, J. A., M. Gong, R. He, M. K. Sgagias, K. H. Dixon, S. L. Anzick, P. S. Meltzer, and K. H. Cowan. 1995. Isolation of a gene encoding a human reduced folate carrier (RFC1) and analysis of its expression in transport-deficient, methotrexate-resistant human breast cancer cells. *Cancer Res.* **55**:3790–3794.
- Nakai, T., H. Mizutani, I. Miyahara, K. Hirotsu, S. Takeda, K. H. Jhee, T. Yoshimura, and N. Esaki. 2000. Three-dimensional structure of 4-amino-4-deoxychorismate lyase from *Escherichia coli*. *J. Biochem.* **128**:29–38.
- Nichols, B. P., A. M. Seibold, and S. Z. Doktor. 1989. para-aminobenzoate synthesis from chorismate occurs in two steps. *J. Biol. Chem.* **264**:8597–8601.
- Parks, L. W. 1978. Metabolism of sterols in yeast. *CRC Crit. Rev. Microbiol.* **6**:301–341.
- Parsons, A. B., R. L. Brost, H. Ding, Z. Li, C. Zhang, B. Sheikh, G. W. Brown, P. M. Kane, T. R. Hughes, and C. Boone. 2004. Integration of

- chemical-genetic and genetic interaction data links bioactive compounds to cellular target pathways. *Nat. Biotechnol.* **22**:62–69.
33. **Parsons, A. B., A. Lopez, I. E. Givoni, D. E. Williams, C. A. Gray, J. Porter, G. Chua, R. Sopko, R. L. Brost, C. H. Ho, J. Wang, T. Ketela, C. Brenner, J. A. Brill, G. E. Fernandez, T. C. Lorenz, G. S. Payne, S. Ishihara, Y. Ohya, B. Andrews, T. R. Hughes, B. J. Frey, T. R. Graham, R. J. Andersen, and C. Boone.** 2006. Exploring the mode-of-action of bioactive compounds by chemical-genetic profiling in yeast. *Cell* **126**:611–625.
 34. **Patel, O. G., E. K. Mberu, A. M. Nzila, and I. G. Macreadie.** 2004. Sulfa drugs strike more than once. *Trends Parasitol.* **20**:1–3.
 35. **Pena-Castillo, L., and T. R. Hughes.** 2007. Why are there still over 1000 uncharacterized yeast genes? *Genetics* **176**:7–14.
 36. **Quevillon, E., V. Silventoinen, S. Pillai, N. Harte, N. Mulder, R. Apweiler, and R. Lopez.** 2005. InterProScan: protein domains identifier. *Nucleic Acids Res.* **33**:W116–W120.
 37. **Quinlivan, E. P., S. Roje, G. Basset, Y. Shachar-Hill, J. F. Gregory III, and A. D. Hanson.** 2003. The folate precursor *p*-aminobenzoate is reversibly converted to its glucose ester in the plant cytosol. *J. Biol. Chem.* **278**:20731–20737.
 38. **Roland, S., R. Ferone, R. J. Harvey, V. L. Styles, and R. W. Morrison.** 1979. The characteristics and significance of sulfonamides as substrates for *Escherichia coli* dihydropteroate synthase. *J. Biol. Chem.* **254**:10337–10345.
 39. **Schagger, H., W. A. Cramer, and G. von Jagow.** 1994. Analysis of molecular masses and oligomeric states of protein complexes by blue native electrophoresis and isolation of membrane protein complexes by two-dimensional native electrophoresis. *Anal. Biochem.* **217**:220–230.
 40. **Tewari, Y. B., P. Y. Jensen, N. Kishore, M. P. Mayhew, J. F. Parsons, E. Eisenstein, and R. N. Goldberg.** 2002. Thermodynamics of reactions catalyzed by PABA synthase. *Biophys. Chem.* **96**:33–51.
 41. **Thompson, J. D., D. G. Higgins, and T. J. Gibson.** 1994. CLUSTAL W: improving the sensitivity of progressive multiple sequence alignment through sequence weighting, position-specific gap penalties and weight matrix choice. *Nucleic Acids Res.* **22**:4673–4680.
 42. **Viswanathan, V. K., J. M. Green, and B. P. Nichols.** 1995. Kinetic characterization of 4-amino 4-deoxychorismate synthase from *Escherichia coli*. *J. Bacteriol.* **177**:5918–5923.
 43. **Wickerham, L. J.** 1951. The classification and taxonomy of yeasts. U.S. Dept. Agric. Tech. Bull. **1029**:1–56.
 44. **Winzeler, E. A., D. D. Shoemaker, A. Astromoff, H. Liang, K. Anderson, B. Andre, R. Bangham, R. Benito, J. D. Boeke, H. Bussey, A. M. Chu, C. Connelly, K. Davis, F. Dietrich, S. W. Dow, M. El Bakkoury, F. Foury, S. H. Friend, E. Gentalen, G. Giaever, J. H. Hegemann, T. Jones, M. Laub, H. Liao, N. Liebundguth, D. J. Lockhart, A. Lucau-Danila, M. Lussier, N. M'Rabet, P. Menard, M. Mittmann, C. Pai, C. Rebischung, J. L. Revuelta, L. Riles, C. J. Roberts, P. Ross-MacDonald, B. Scherens, M. Snyder, S. Sookhai-Mahadeo, R. K. Storms, S. Veronneau, M. Voet, G. Volckaert, T. R. Ward, R. Wysocki, G. S. Yen, K. Yu, K. Zimmermann, P. Philippens, M. Johnston, and R. W. Davis.** 1999. Functional characterization of the *Saccharomyces cerevisiae* genome by gene deletion and parallel analysis. *Science* **285**:901–906.
 45. **Yadav, J., S. Muend, Y. Zhang, and R. Rao.** 2007. A phenomics approach in yeast links proton and calcium pump function in the Golgi. *Mol. Biol. Cell* **18**:1480–1489.